J. Fluid Mech. (1970), *vol.* 41, *part* 3, *pp.* 673–687
Printed in Great Britain

An unsteady two-cell vortex solution of the Navier–Stokes equations

By P. G. BELLAMY-KNIGHTS
Department of the Mechanics of Fluids, University of Manchester

(Received 27 July 1969)

The steady two-cell viscous vortex solution of Sullivan (1959) is extended to yield unsteady two-cell viscous vortex solutions which behave asymptotically as certain analogous unsteady one-cell solutions of Rott (1958). The radial flux is a parameter of the solution, and the effect of the radial flow on the circumferential velocity, is analyzed. The work suggests an explanation for the eventual dissipation of meteorological flow systems such as tornadoes.

1. Introduction

The diffusion of an unsteady viscous vortex with zero radial and axial velocity components is well understood. Physical flows, however, are characterized by non-zero radial and axial velocity components due to the existence of boundaries such as a plane wall perpendicular to the axis of symmetry of the vortex. The work presented here is designed to obtain additional solutions containing radial and axial velocity components and to analyze their effect on the swirl and on the diffusion of the vorticity.

The present stagnation point flow solution was developed during an analytical investigation of the axial flow reversal phenomenon in the core of a viscous vortex subsequent to vortex breakdown. First, this work is of mathematical interest in providing an exact solution of the full incompressible unsteady axisymmetric Navier–Stokes equations. Secondly, it belongs to a class of solutions

$$u = u(r,t), \quad v = v(r,t), \quad w = zW(r,t), \tag{1.1}$$

which has been found useful in modelling geophysical vortices (Morton 1966); here r and z are cylindrical polar co-ordinates, u, v and w are the radial, tangential and axial components of velocity respectively and t is the time. Solutions of this type do not permit any lateral expansion of the vortex core with height, they only satisfy the inviscid boundary conditions on the ground, $z = 0$, and they have the limitation that vertical velocities increase indefinitely in magnitude with increasing height. They may, however, be used to represent the core flow in the axial region where the boundary-layer effects of the ground and the lateral core expansion can be neglected.

In the case

$$W(r,t) = 0 \tag{1.2}$$

Oseen (1911) obtained the well-known unsteady solution of this class which is

$$u = 0, \quad v = \frac{K_c}{r}\left[1-\exp\left(-\frac{r^2}{4\nu t}\right)\right], \quad w = 0, \tag{1.3}$$

K_c determines the circulation and ν is the kinematic viscosity. This solution describes the process of decay, through the action of viscosity, of a vortex filament which is concentrated at the origin at $t = 0$. $2\pi K_c$ is the initial value of the circulation about the origin.

Subsequently, Burgers (1940, 1948) and Rott (1958, 1959) independently obtained a steady solution for a viscous vortex embedded in a radially inward axisymmetric stagnation point flow over a plane boundary in the form

$$\left.\begin{aligned} u &= -ar, \quad v = \frac{K_c}{r}\left[1-\exp\left(-\frac{ar^2}{2\nu}\right)\right], \quad w = 2az, \\ p &= p_0 - \tfrac{1}{2}\rho(4a^2z^2+a^2r^2)+\rho\int_0^r v^2 r^{-1}\,dr, \end{aligned}\right\} \tag{1.4}$$

where a is a constant related to the core diameter and p_0 is the stagnation point pressure.

A two-cell solution, characterized by axial flow reversal along and near the axis of the vortex, was obtained by Sullivan (1959):

$$\left.\begin{aligned} u &= -ar + \frac{6\nu}{r}\left[1-\exp\left(-\frac{ar^2}{2\nu}\right)\right], \\ v &= \frac{K_c}{r}\left[H\left(\frac{ar^2}{2\nu}\right)\Big/H(\infty)\right], \\ w &= 2az\left[1-3\exp\left(-\frac{ar^2}{2\nu}\right)\right], \\ p &= p_0 - \tfrac{1}{2}\rho\left\{4a^2z^2+a^2r^2+36(\nu^2/r^2)\left[1-\exp\left(-\frac{ar^2}{2\nu}\right)\right]^2\right\}+\rho\int_0^r v^2 r^{-1}\,dr, \end{aligned}\right\} \tag{1.5}$$

where H is defined by

$$H(x) = \int_0^x \exp\left\{-t+3\int_0^t [1-\exp(-s)]\,s^{-1}\,ds\right\}dt.$$

For large values of r, the velocity and pressure reduce to the values given by Burgers' solution. This outer flow, consisting of spiralling inward radial flow and upward axial flow, is separated from an inner flow by a cylindrical stream tube. The inner flow consists of a spiralling flow which is downwards near the axis and radially outwards and then upwards near the separation surface.

In this paper, Sullivan's solution is generalized to provide a two-cell solution in which the separation surface between the two cells moves radially outwards with a velocity related to the diffusion of the vorticity.

The mathematical procedure is as follows. The pressure is eliminated from the radial and axial momentum equations to yield a third-order non-linear partial differential equation for the stream function. The solution to the steady-flow problem suggests the form of solution in the unsteady case. Certain constant coefficients in the steady-flow solution are replaced by suitable functions of time. It is assumed that the circulation is a function of a similarity variable which is in turn a function of r and t. This similarity variable is suggested by the form of the solution for the stream function. These considerations reduce the problem to solving three first-order ordinary differential equations for the time dependent coefficients in the stream function. Sullivan's steady-flow solution is obtained as a special case.

It is also shown that, for large values of r, the unsteady two-cell solution asymptotically behaves in the same way as the analogous one-cell unsteady solution considered by Rott (1958).

2. Mathematical formulation of the problem

The analysis starts with the full Navier–Stokes equations for the unsteady axisymmetric flow of an incompressible fluid

$$\frac{\partial u}{\partial t}+u\frac{\partial u}{\partial r}+w\frac{\partial u}{\partial z}-\frac{v^2}{r}=-\frac{1}{\rho}\frac{\partial p}{\partial r}+\nu\left[\frac{\partial^2 u}{\partial r^2}+\frac{1}{r}\frac{\partial u}{\partial r}-\frac{u}{r^2}+\frac{\partial^2 u}{\partial z^2}\right], \tag{2.1a}$$

$$\frac{\partial v}{\partial t}+u\frac{\partial v}{\partial r}+w\frac{\partial v}{\partial z}+\frac{uv}{r}=\nu\left[\frac{\partial^2 v}{\partial r^2}+\frac{1}{r}\frac{\partial v}{\partial r}-\frac{v}{r^2}+\frac{\partial^2 v}{\partial z^2}\right], \tag{2.1b}$$

$$\frac{\partial w}{\partial t}+u\frac{\partial w}{\partial r}+w\frac{\partial w}{\partial z}=-\frac{1}{\rho}\frac{\partial p}{\partial z}+\nu\left[\frac{\partial^2 w}{\partial r^2}+\frac{1}{r}\frac{\partial w}{\partial r}+\frac{\partial^2 w}{\partial z^2}\right], \tag{2.1c}$$

together with the continuity equation

$$\frac{\partial u}{\partial r}+\frac{u}{r}+\frac{\partial w}{\partial z}=0. \tag{2.1d}$$

These equations are to be solved by seeking a solution of the form given in (1.1). The boundary conditions to be satisfied are that the radial and circumferential velocities on the axis of symmetry are zero and that the circulation approaches a constant value, $2\pi K_c$, as the radial distance increases.

For convenience, a function $g(r,t)$ is introduced such that $2\pi g$ is the outflux of fluid, per unit axial length, across a cylinder of radius r with its axis of symmetry coincidental with the z axis. Then

$$u = g/r \tag{2.2a}$$

and

$$g = \partial g/\partial r = 0 \quad \text{when} \quad r = 0 \tag{2.2b}$$

in order to satisfy the boundary conditions for the radial velocity on the axis of the vortex. The continuity equation (2.1d) then gives

$$w=-\frac{z}{r}\frac{\partial g}{\partial r}. \tag{2.3}$$

From the radial and axial momentum equations, (2.1a) and (2.1c) respectively, it is found that

$$\frac{1}{\rho}\frac{\partial p}{\partial r}=\frac{\partial}{\partial r}\left(\frac{\nu}{r}\frac{\partial g}{\partial r}-\frac{1}{2}\frac{g^2}{r^2}\right)-\frac{1}{r}\frac{\partial g}{\partial t}+\frac{v^2}{r} \tag{2.4}$$

and

$$\frac{1}{\rho}\frac{\partial p}{\partial z}=z\left\{-\frac{\nu}{r}\frac{\partial}{\partial r}\left[r\frac{\partial}{\partial r}\left(\frac{1}{r}\frac{\partial g}{\partial r}\right)\right]+\frac{1}{r}\frac{\partial^2 g}{\partial r\,\partial t}+\frac{g}{r}\frac{\partial}{\partial r}\left(\frac{1}{r}\frac{\partial g}{\partial r}\right)-\left(\frac{1}{r}\frac{\partial g}{\partial r}\right)^2\right\}. \tag{2.5}$$

Now the right-hand side of (2.4) is a function of r and t only and so

$$\frac{\partial^2 p}{\partial r\,\partial z} = 0. \tag{2.6}$$

Thus (2.5) can be written as

$$\frac{1}{\rho}\frac{\partial p}{\partial z} = zF_1(t), \tag{2.7}$$

where $F_1(t)$ is determined by the outflux. Comparison of (2.5) and (2.7) provides a differential equation for g which can be simplified by the transformation

$$x = r^2 \tag{2.8}$$

to give

$$-2\nu\frac{\partial}{\partial x}\left(x\frac{\partial^2 g}{\partial x^2}\right)+g\frac{\partial^2 g}{\partial x^2}-\left(\frac{\partial g}{\partial x}\right)^2+\frac{1}{2}\frac{\partial^2 g}{\partial x\,\partial t} = \tfrac{1}{4}F_1(t). \tag{2.9}$$

The circumferential momentum equation is

$$\frac{\partial K}{\partial t}+\frac{g}{r}\frac{\partial K}{\partial r} = \nu r\frac{\partial}{\partial r}\left(\frac{1}{r}\frac{\partial K}{\partial r}\right), \tag{2.10}$$

where $2\pi K$ is the circulation.

A similarity solution for K is now considered by transforming from (r,t) co-ordinates to (η,t) co-ordinates where

$$\eta = \eta(r,t) \tag{2.11}$$

is some as yet unspecified similarity variable. Then K is a function of η only, which is specified by the equation

$$\frac{d^2K}{d\eta^2}+\alpha(\eta)\frac{dK}{d\eta} = 0, \tag{2.12}$$

provided that $\alpha(\eta)$ satisfies

$$r\nu\frac{\partial}{\partial r}\left(\frac{1}{r}\frac{\partial \eta}{\partial r}\right)-\frac{\partial \eta}{\partial t}-\frac{g}{r}\frac{\partial \eta}{\partial r} = \alpha(\eta)\,\nu\left(\frac{\partial \eta}{\partial r}\right)^2. \tag{2.13}$$

The function $\alpha(\eta)$ is to be obtained such that the boundary conditions for the circulation can be satisfied. In terms of the (x,t) co-ordinates, (2.13) reduces to

$$4\nu x\frac{\partial^2 \eta}{\partial x^2}-\frac{\partial \eta}{\partial t}-2g\frac{\partial \eta}{\partial x} = 4\nu x\,\alpha(\eta)\left(\frac{\partial \eta}{\partial x}\right)^2. \tag{2.14}$$

A solution can now be obtained by the following steps. Equation (2.9) is solved for g and hence the radial and axial velocity components are given by (2.2a) and (2.3) respectively. Since g occurs in the differential equation (2.13), the form of the solution for g may suggest the choice of the r dependence of the similarity variable η so that (2.13) will give α explicitly. Then (2.12) can be solved for the circulation K and finally (2.4) and (2.7) will give the pressure.

3. Solutions for special cases

(a) One-cell solutions

It is readily seen that one solution of (2.9) which satisfies boundary conditions (2.2) is

$$g = xa(t), \tag{3.1}$$

where
$$\frac{da}{dt} - 2a^2 - \tfrac{1}{2}F_1(t) = 0. \tag{3.2}$$
Hence from (2.3) and (2.8)
$$w = -2za(t). \tag{3.3}$$
In this case it is seen that the axial velocity is independent of r. Thus the flow can be envisaged as taking place between two parallel frictionless planes perpendicular to the axis of symmetry so that
$$w = 0 \quad \text{on} \quad z = 0 \qquad \text{and} \qquad w = dH/dt \quad \text{on} \quad z = H(t), \tag{3.4}$$
where H is the time-dependent separation distance between the planes. Thus $a(t)$ and $F_1(t)$ are specified in terms of $H(t)$. One solution of equation (2.14) leading to Rott's (1958) unsteady one-cell solutions is
$$\eta = xC(t), \tag{3.5}$$
where
$$C(t) = \frac{H(t)}{4\nu\alpha\int H(t)\,dt + \beta'} \tag{3.6}$$
and α and β' are constants. Hence, from (2.12) it is found that
$$K = K_c\left[1 - \exp\left\{\frac{-r^2}{4\nu}\left(\frac{H(t)}{\int H(t)\,dt + \beta}\right)\right\}\right], \tag{3.7}$$
where
$$\beta' = 4\nu\alpha\beta. \tag{3.8}$$

If H is constant, then Oseen's (1911) unsteady viscous vortex, given in (1.3), is obtained. If
$$H = A\exp(mt),$$
where A and m are constants, then Burgers' (1940) steady viscous vortex solution results.

(b) *Two-cell solutions*

A solution of the form
$$g = a(t)x + b(t)\,[1 - \exp(-c(t)x)] \tag{3.9}$$
is now considered. Substituting this value of g into (2.9) and equating the coefficients of $x\exp(-cx)$, $\exp(-cx)$ and terms independent of x to zero yield the following equations for $a(t)$, $b(t)$ and $c(t)$:
$$\frac{dc}{dt} + 2ac + 4\nu c^2 = 0, \tag{3.10}$$
$$\frac{db}{dt} - 6ab - 2b^2c = 0, \tag{3.11}$$
$$\frac{da}{dt} - 2a^2 - \tfrac{1}{2}F_1(t) = 0. \tag{3.12}$$

The value of the similarity variable suggested by the form of g is
$$\eta = c(t)x. \tag{3.13}$$

Substitution of (3.9) and (3.13) into (2.14) yields

$$-\frac{dc/dt+2ac}{c^2}-\frac{2b}{cx}[1-\exp(-cx)] = 4\nu\alpha.$$

Dividing by 4ν and using (3.10) and (3.13) reduce the above equation to

$$\alpha = 1-\frac{b}{2\nu\eta}[1-\exp(-\eta)]. \tag{3.14}$$

Thus for α to be a function of η only, b must be a constant. This constant, b, is now taken as non-zero as otherwise the solution would reduce to the class of one-cell solutions already considered. Equation (3.11) now yields

$$a = -\tfrac{1}{3}bc(t). \tag{3.15}$$

Equations (3.10) and (3.15) give

$$c^{-2}\frac{dc}{dt} = -\lambda, \tag{3.16}$$

where

$$\lambda = \tfrac{2}{3}(6\nu-b). \tag{3.17}$$

Integration gives

$$c = \frac{1}{\lambda t+\mu}, \tag{3.18}$$

where μ is a constant.

Hence, from (3.13), (2.8) and (3.18)

$$\eta = \frac{r^2}{\lambda t+\mu}. \tag{3.19}$$

Equations (3.9), (3.18) and (3.15) yield

$$g = -\frac{b}{3}\left(\frac{r^2}{\lambda t+\mu}\right)+b\left(1-\exp\left[\frac{-r^2}{\lambda t+\mu}\right]\right). \tag{3.20}$$

Hence, using (2.2a) and (2.3),

$$u = -\frac{b}{3}\left(\frac{r}{\lambda t+\mu}\right)+\frac{b}{r}\left(1-\exp\left[\frac{-r^2}{\lambda t+\mu}\right]\right) \tag{3.21}$$

and

$$w = z\left\{\frac{2b}{3}\left(\frac{1}{\lambda t+\mu}\right)-\frac{2b}{\lambda t+\mu}\exp\left[\frac{-r^2}{\lambda t+\mu}\right]\right\}. \tag{3.22}$$

The circulation is now obtained by solving (2.12) where α is given by (3.14). The solution is

$$K = K_c\frac{\mathscr{H}_{b/2\nu}(\eta)}{\mathscr{H}_{b/2\nu}(\infty)}, \tag{3.23}$$

where

$$\mathscr{H}_m(s) = \int_0^s \exp\left[-y+m\int_0^y\left(\frac{1-e^{-q}}{q}\right)dq\right]dy. \tag{3.24}$$

From (2.4) and (2.5), the pressure is obtained given by

$$\frac{p}{\rho} = \frac{bz^2}{(\lambda t+\mu)^2}\left(\frac{\lambda}{3}-\frac{2b}{9}\right)-\frac{br^2}{18(\lambda t+\mu)^2}(3\lambda+b)$$
$$-\frac{b^2}{2r^2}\left(1-\exp\left[\frac{-r^2}{\lambda t+\mu}\right]\right)^2+\int_0^r\frac{v^2}{r}dr+\frac{p_0(t)}{\rho}, \tag{3.25}$$

where $p_0(t)$ is the pressure at the stagnation point.

For large values of r, the velocity components and pressure tend asymptotically to the corresponding values given by Rott's unsteady one-cell vortex for which

$$H(t) = C(\lambda t+\mu)^{2b/3\lambda}, \tag{3.26}$$

where C is a constant. These asymptotic values are

$$u = -\frac{br}{3(\lambda t+\mu)}, \tag{3.27}$$

$$w = \frac{2bz}{3(\lambda t+\mu)}, \tag{3.28}$$

$$v = \frac{K_c}{r}\left(1-\exp\left[\frac{-r^2}{\lambda t+\mu}\right]\right), \tag{3.29}$$

$$\frac{p}{\rho} = \frac{bz^2}{(\lambda t+\mu)^2}\left(\frac{\lambda}{3}-\frac{2b}{9}\right)-\frac{br^2}{18(\lambda t+\mu)^2}(3\lambda+b)+\int_0^r\frac{v^2}{r}dr+\frac{p_0(t)}{\rho}. \tag{3.30}$$

Now when $$b = 6\nu \tag{3.31}$$

(3.17) gives $$\lambda = 0. \tag{3.32}$$

Then if $$\mu = \frac{2\nu}{a}, \tag{3.33}$$

(3.21), (3.22), (3.23) and (3.25) reduce to (1.5) giving Sullivan's (1959) steady two-cell solution. Similarly, equations (3.27), (3.28), (3.29) and (3.30) reduce to (1.4) giving Burgers' (1940) steady one-cell solution.

If $$\lambda \neq 0,$$

μ can always be arranged to be zero by effecting a change in the zero of the time-scale. Thus, in the remainder of this work it will be assumed that

$$\mu = 0, \tag{3.34}$$

unless it is stated otherwise.

Here, it can be noted that when

$$b = 0, \tag{3.35}$$

(3.17) gives $$\lambda = 4\nu$$

and (3.24) gives $$\mathscr{H}_0(s) = 1-e^{-s}.$$

In this case, (3.21), (3.22) and (3.23) reduce to (1.3) giving Oseen's (1911) solution.

In order to simplify the discussion of the general solution, the variables will be made dimensionless in terms of ν, K_c and radial and axial length scales r_0 and z_0 respectively. Thus dimensionless variables $\bar{r}$, $\bar{z}$, $\bar{t}$, $\bar{u}$, $\bar{v}$, $\bar{w}$, ξ, $\bar{b}$ and $\bar{\lambda}$ are introduced, defined by

$$(\bar{r},\bar{z}) = \left(\frac{r}{r_0},\frac{z}{z_0}\right), \tag{3.36, 37}$$

$$\bar{t} = \frac{4\nu t}{r_0^2}, \tag{3.38}$$

$$(\bar{u},\bar{w}) = \frac{r_0}{2\nu}(u,w), \tag{3.39, 40}$$

$$\bar{v} = \frac{r_0 v}{K_c}, \tag{3.41}$$

$$\xi = \frac{2z_0}{r_0}, \tag{3.42}$$

$$\bar{b} = \frac{b}{2\nu}, \tag{3.43}$$

$$\bar{\lambda} = \frac{\lambda}{4\nu}. \tag{3.44}$$

Then (3.17) becomes
$$\bar{\lambda} = 1 - \tfrac{1}{3}\bar{b} \tag{3.45}$$

and (3.19) becomes
$$\eta = \frac{\bar{r}^2}{\bar{t}[1-\frac{1}{3}\bar{b}]}. \tag{3.46}$$

Equations (3.21), (3.22), (3.23) give

$$\bar{u} = \left(\frac{-\bar{b}}{3-\bar{b}}\right)\frac{\bar{r}}{\bar{t}} + \frac{\bar{b}}{\bar{r}}\left(1 - \exp\left[\frac{-\bar{r}^2}{\bar{t}(1-\frac{1}{3}\bar{b})}\right]\right), \tag{3.47}$$

$$\bar{w} = \left(\frac{\bar{b}\xi}{3-\bar{b}}\right)\frac{\bar{z}}{\bar{t}}\left(1 - 3\exp\left[\frac{-\bar{r}^2}{\bar{t}(1-\frac{1}{3}\bar{b})}\right]\right), \tag{3.48}$$

$$\bar{v} = \frac{1}{\bar{r}}\mathscr{H}_{\bar{b}}\left(\frac{\bar{r}^2}{\bar{t}(1-\frac{1}{3}\bar{b})}\right)\Big/\mathscr{H}_{\bar{b}}(\infty). \tag{3.49}$$

Similarly, the asymptotic values given in (3.27), (3.28) and (3.29) become

$$\bar{u} = \frac{-\bar{b}\bar{r}}{(3-\bar{b})\bar{t}}, \tag{3.50}$$

$$\bar{w} = \frac{\bar{b}\xi\bar{z}}{(3-\bar{b})\bar{t}}, \tag{3.51}$$

$$\bar{v} = \frac{1}{\bar{r}}\left(1 - \exp\left[\frac{-\bar{r}^2}{\bar{t}(1-\frac{1}{3}\bar{b})}\right]\right). \tag{3.52}$$

4. Discussion of results

(a) The radial and axial velocity components

It is seen from (3.46) and (3.47) that

$$\bar{u} = 0$$

when
$$\eta = 3(1-e^{-\eta}),$$

that is, when
$$\eta = 2{\cdot}821 = \eta_1, \quad \text{say.} \tag{4.1}$$

The flow can be regarded as being divided into two cells separated by the time-dependent cylindrical surface given by

$$\eta = \eta_1.$$

The radial velocity in one cell is in the opposite direction to that in the other cell. From (3.48) it is seen that there is another time-dependent cylindrical surface in the inner cell, at which the axial velocity is zero. This is given by

$$\eta = \log_e 3 = \eta_0, \quad \text{say.} \tag{4.2}$$

The effects of the radial flow parameter, $\bar{b}$, will now be considered with the help of figure 1, in which the similarity variable parameter, $\bar{\lambda}$, is plotted as a function of $\bar{b}$ using (3.45). When

$$\bar{b} > 0$$

it can be seen from (3.47) and (3.48) that the flow in the outer cell consists of radial inflow and axial upflow. In the inner cell there is radial outflow accom-

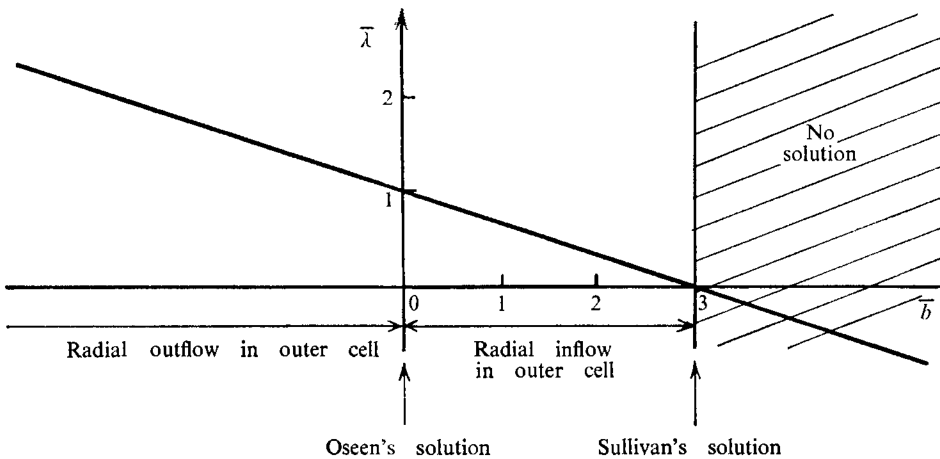

FIGURE 1. The similarity variable parameter plotted as a function of the radial flow parameter.

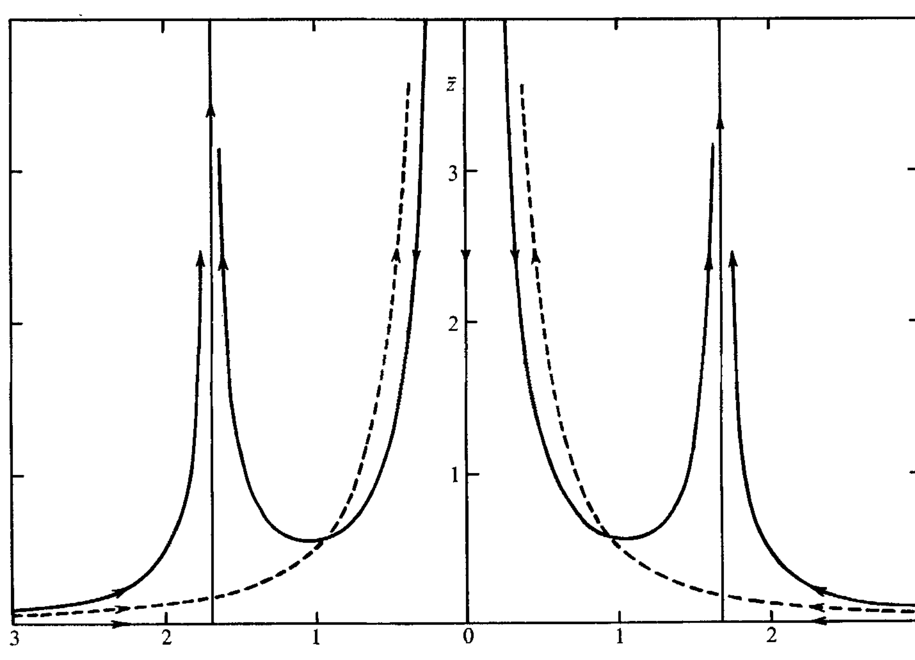

FIGURE 2. The stream surfaces when $\bar{t} = 3$ and $\bar{b} = 2$ for the two-cell solution (solid lines) and the corresponding one-cell solution (broken lines).

panied by axial flow which is either downwards or upwards according as $\eta \lesseqgtr \eta_0$. These features are illustrated in figure 2 which shows the instantaneous traces of certain stream surfaces in a meridian plane for a specified value of $\bar{b}$.

Now in order to satisfy the boundary condition that the circulation tends to a constant value as the radius tends to infinity, it is required that $\bar{\lambda} \geqslant 0$ (where $\mu \neq 0$ when $\bar{\lambda} = 0$). Hence, from figure 1, there are no solutions when $\bar{b} > 3$. As will be discussed later, a physical characteristic of flows for which $\bar{b}$ is greater than three is that the convection of fresh circulation into the vortex core due to the radial inflow of the outer cell would predominate over the process of the diffusion

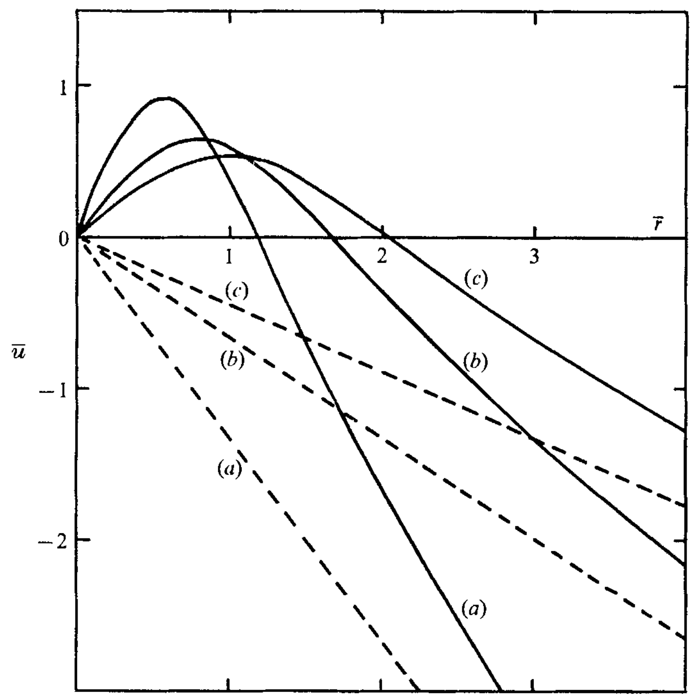

FIGURE 3. The radial velocity distribution when $\bar{b} = 2$ for the two-cell solution (solid lines) and the corresponding one-cell solution (broken lines): $\bar{t}$ = 1·5, 3 and 4·5, respectively, for curves (*a*), (*b*) and (*c*).

of the vorticity. The limiting case for possible solutions, namely $\bar{b} = 3$ corresponds to Sullivan's steady flow solution. It may be noted that all flows for which $\bar{b} < 3$ are unsteady flows.

When $\bar{b} < 0$ the flow in the outer cell consists of radial outflow and axial downflow. In the inner cell there is radial inflow accompanied by axial flow which is either upwards or downwards according as $\eta \lesseqgtr \eta_0$. Thus the flow pattern at any instant is similar to that shown in figure 2, the main difference being that the direction of flow is everywhere reversed. It should, however, be noted that the stream surfaces when $\bar{t} = 3$ and $\bar{b} = -2$ will not quantitatively be the same as those represented in figure 2 for $\bar{b} = 2$ since from figure 1, it is seen that $\bar{\lambda}$ is not symmetric about the line $\bar{b} = 0$. In fact, for the former flow, the value of $\bar{\lambda}$ will be larger than for the latter flow, and so, for the former flow, the dividing cylinder between the two cells will expand at a greater rate.

Figure 3 traces the development of the radial velocity with time from (3.47) with

$$\bar{b} = 2. \tag{4.3}$$

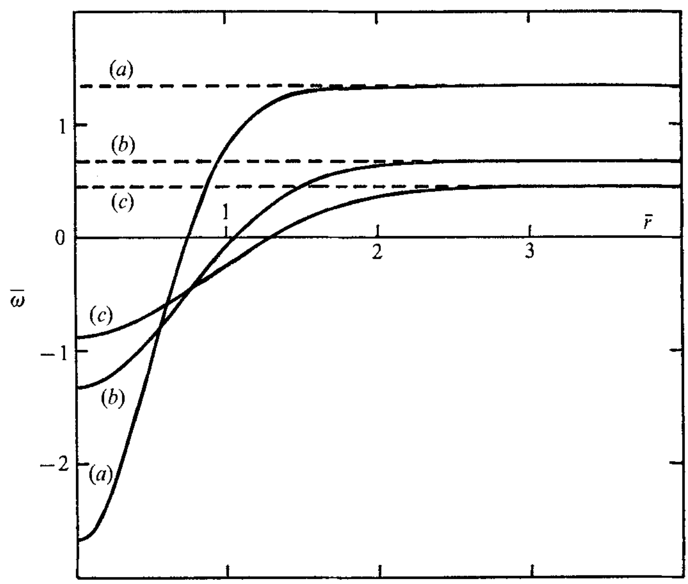

FIGURE 4. The axial velocity distribution when $\bar{b} = 2$ and $\bar{z} = 1$ for the two-cell solution (solid lines) and the corresponding one-cell solution (broken lines): $\bar{t} = 1{\cdot}5$, 3 and $4{\cdot}5$, respectively, for curves (a), (b) and (c).

As time increases, the bounding surface between the two cells expands radially. The non-dimensional radius of this bounding surface, $\bar{r}_1$ say, is given as a function of time by

$$\bar{r}_1^2 = \eta_1[1 - \tfrac{1}{3}\bar{b}]\,\bar{t},$$

reducing to

$$\bar{r}_1 = 0{\cdot}970(\bar{t})^{\frac{1}{2}}$$

using (3.46), (4.1) and (4.3).

For the same value of $\bar{b}$ and at a fixed (non-zero) axial plane, figure 4 traces the development of the axial velocity with time from (3.48). Accompanying the radial expansion of the inner cell, is the expansion of the radius, non-dimensionalized as $\bar{r}_0$ say, of the cylindrical surface on which the axial velocity is zero. This is given by

$$\bar{r}_0^2 = \eta_0[1 - \tfrac{1}{3}\bar{b}]\,\bar{t},$$

reducing to

$$\bar{r}_0 = 0{\cdot}605(\bar{t})^{\frac{1}{2}},$$

using (3.46), (4.2) and (4.3).

Figures 3 and 4 show that the maximum radial and axial velocities in the inner cell decrease as time increases. Also plotted in these figures are the corresponding asymptotic values of the velocities specified by the appropriate one-cell solution of Rott given in equations (3.50) and (3.51).

It has already been observed that the maximum value of $\bar{b}$, which yields a solution satisfying the boundary condition for the circulation at infinity, is three. In this case the solution is independent of time with the bounding surface between the two cells maintained at a constant radius. This steady motion is possible because the diffusion of the vorticity due to viscosity is balanced by the convection of fresh circulation from outside the vortex core due to the radial inflow. When $\bar{b} < 3$ this radial inflow from the outer cell is reduced thus causing

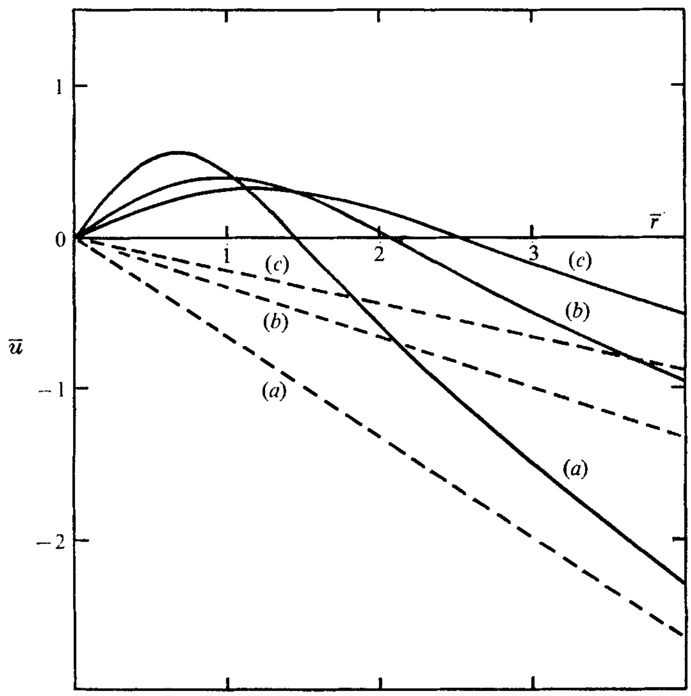

FIGURE 5. The radial velocity distribution when $\bar{b} = 1{\cdot}5$ for the two-cell solution (solid lines) and the corresponding one-cell solution (broken lines): $\bar{t} = 1{\cdot}5$, 3 and $4{\cdot}5$, respectively, for curves (*a*), (*b*) and (*c*).

the diffusion process to predominate. This results in unsteady flows for which the inner cell expands with time as already described. As $\bar{b}$ decreases, so the diffusion process becomes increasingly predominant with the result that if the graphs for the radial and axial velocities for two differing values of $\bar{b}$, but at the same time, are compared, then it is seen that the inner cell for the lower value of $\bar{b}$ is expanding at a greater rate than for the higher value of $\bar{b}$. Comparison of figures 3 and 5 illustrate this.

(*b*) *The circumferential velocity component*

A typical circumferential velocity distribution for any value of $\bar{b}$ and at any time consists of an inner core region in which the swirl velocity increases from zero on the axis of symmetry to a maximum value and for which the circumferential flow resembles that due to a rigid body rotation. Outside this core region the swirl velocity decreases and tends asymptotically to the value given by a potential vortex. As time increases the vortex diffuses with the result that the swirl at all finite radial positions decreases and the radial position of the point of maximum swirl increases. These general observations are illustrated in figures 6–8 in which the circumferential velocity is plotted using (3.49) for three values of $\bar{b}$. For each value of $\bar{b}$, the swirl is plotted at three different times. For each of these curves, the corresponding circumferential velocity distribution curve for the Oseen vortex, $\bar{b} = 0$ is also plotted for purposes of comparison.

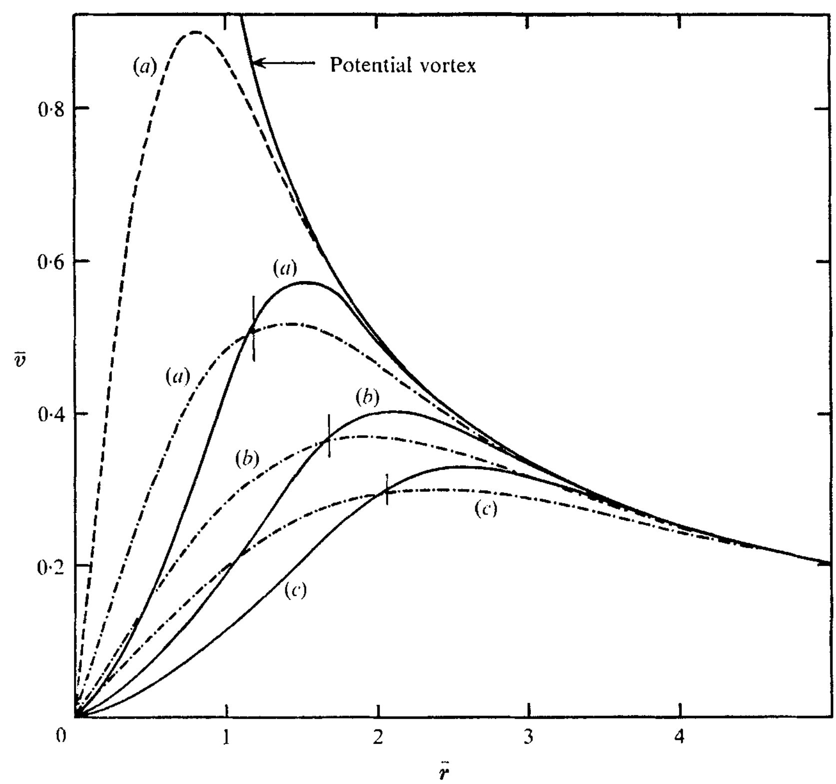

FIGURE 6. The circumferential velocity distribution for the two-cell solution for which $\bar{b} = 2$ (solid lines), the corresponding one-cell solution for which $\bar{b} = 2$ (broken lines of type -----) and for the Oseen solution for which $\bar{b} = 0$ (broken lines of type –·–·–): $\bar{t}$ = 1·5, 3 and 4·5, respectively, for curves (*a*), (*b*) and (*c*).

The effect of the radial flow on the swirl may be discussed with reference to figure 6 in which $\bar{b} = 2$. At any time, the effect of the radial inflow in the outer cell is to increase the swirl in the outer cell over that pertaining to the Oseen vortex at the same radius and time. On the other hand, the radial outflow in the inner cell has the opposite effect and so gives a lower value of swirl than would pertain for the Oseen vortex. This results in the two-cell velocity profile becoming concave upwards. When $\bar{b} = 2$ the point of intersection of the circumferential velocity distribution curve with the corresponding curve at the same time for the Oseen vortex corresponds to the radial position at which $\bar{u} = 0$ at that time given in figure 3. These latter radial positions are indicated in figure 6 by short vertical strokes. The short vertical strokes in figures 7 and 8 have similar meanings. Also plotted in figure 6 is the swirl distribution for the corresponding one-cell

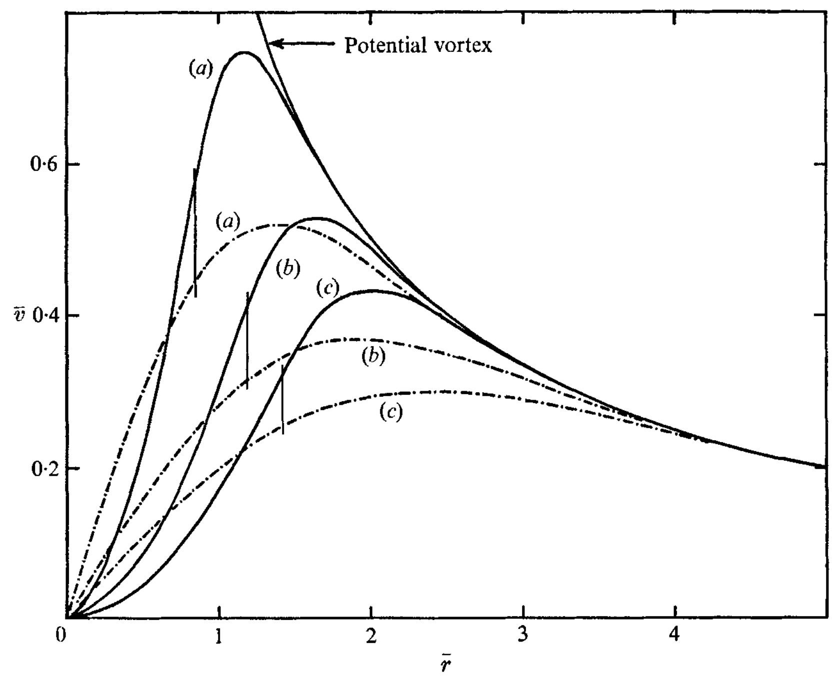

FIGURE 7. The circumferential velocity distribution for the two-cell solution for which $\bar{b} = 2{\cdot}5$ (solid lines) and for the Oseen solution for which $\bar{b} = 0$ (broken lines): $\bar{t} = 1{\cdot}5$, 3 and 4·5, respectively, for curves (*a*), (*b*) and (*c*).

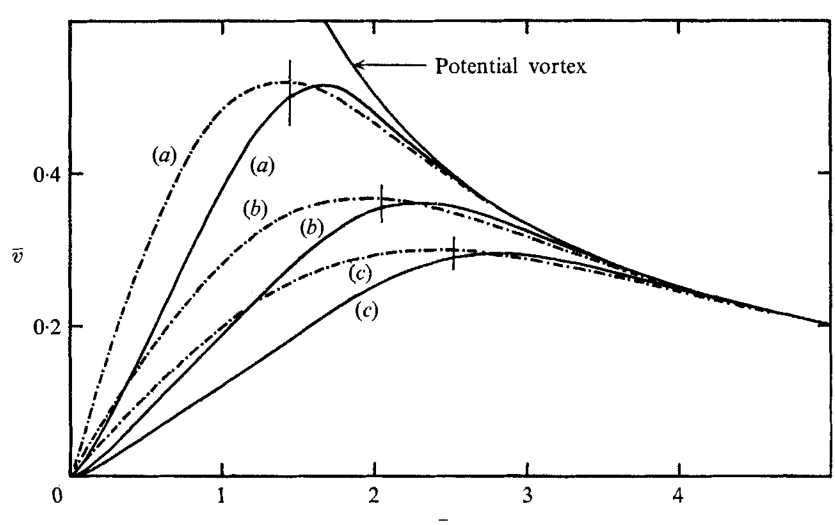

FIGURE 8. The circumferential velocity distribution for the two-cell solution for which $\bar{b} = 1{\cdot}5$ (solid lines) and for the Oseen solution for which $\bar{b} = 0$ (broken lines): $\bar{t} = 1{\cdot}5$, 3 and 4·5, respectively, for curves (*a*), (*b*) and (*c*).

unsteady solution of Rott when $\bar{t} = \frac{3}{2}$ given by (3.52). As is expected, since there is radial inflow throughout the vortex, the swirl at all radial positions is higher than that associated with the two-cell or Oseen vortices. This characteristic holds for all time and for all values of $\bar{b}$.

With reference to figure 7, it is seen that for a larger value of $\bar{b}$, the inflow process in the outer cell predominates over the outflow process in the inner cell with the result that in the outer part of the inner cell the swirl is greater than that for the Oseen vortex. This is due to the viscous shearing in the circumferential direction across the surface dividing the two cells. With reference to figure 8, it can be seen that the reverse of this phenomenon occurs when $\bar{b} < 2$.

5. Conclusions

The above work suggests an explanation for the eventual dissipation of tornadoes and similar meteorological phenomena as represented by Sullivan's steady solution. An essential feature of the steady two-cell solution is that the reduction in circumferential velocity at any radius due to the diffusion of the vorticity should be balanced by the circumferential velocity increase resulting from the inwards convection of fluid with higher angular momentum. Now as soon as the radial inflow ceases to be maintained the diffusion process will predominate thus causing the magnitudes of the swirl velocities to decrease with time as the vortex diffuses. Even for a value of $\bar{b}$ just less than three, the unsteady solution will hold leading to the eventual dissolution of the vortex with time. As has been discussed by Morton (1966), the axial flow (and hence by continuity the radial flow) can be regarded as controlled by thermal effects yielding buoyancy forces. This provides a possible basis for the choice of $\bar{b}$.

A noteworthy mathematical feature of the present work is the way in which the exact choice of the similarity variable is left until towards the end of the solution and that it is found to vary linearly, passing through the values it would have for the Oseen and Sullivan vortices.

The author is indebted to Professor N. H. Johannesen in whose department this work was done and to Dr I. M. Hall under whose guidance this paper was produced. During the course of this work the author was in receipt of a Research Studentship from the Science Research Council.

REFERENCES

Burgers, J. M. 1940 Application of a model system to illustrate some points of the statistical theory of free turbulence. *Proc. Acad. Sci. Amst.* **43**, 2.

Burgers, J. M. 1948 A mathematical model illustrating the theory of turbulence. *Adv. appl. Mech.* **1**, 197.

Morton, B. R. 1966 Geophysical vortices. *Progress in Aeronautical Sciences*, **7**, 145.

Oseen, C. W. 1911 *Ark. Mat. Astr. Fys.* **7**.

Rott, N. 1958 On the viscous core of a line vortex. *Z.A.M.P.* **9***b*, 543.

Rott, N. 1959 On the viscous core of a line vortex II. *Z.A.M.P.* **10**, 73.

Sullivan, R. D. 1959 A two-cell solution of the Navier–Stokes equations. *J. Aero/Space Sci.* **26**, 767.